Available online at www.sciencedirect.com
ScienceDirect
Journal of Molecular Graphics and Modelling 26 (2007) 634–642
Journal of Molecular Graphics and Modelling
www.elsevier.com/locate/JMGM

Drug design: New inhibitors for HIV-1 protease based on Nelfinavir as lead

M.A.S. Perez, P.A. Fernandes, M.J. Ramos *

REQUIMTE, Faculdade de Ciências, Universidade do Porto, Rua do Campo Alegre, 687, 4169-007 Porto, Portugal

Accepted 20 March 2007
Available online 24 March 2007

Abstract

Nelfinavir (Viracept®) is a potent, non-peptidic inhibitor of HIV-1 Protease, which has been marketed for the treatment of HIV infected patients. However, HIV-1 develops drug-resistance which decreases the affinity of Nelfinavir for the binding pocket of Protease. We present here three new variants of Nelfinavir, which we have designed with computational tools, with greater affinity for HIV-1 Protease than Nelfinavir itself. Accordingly, we have introduced rational modifications in Nelfinavir, optimizing its affinity to the most conserved amino acids in Protease, in order to increase the efficiency of the three new inhibitors.

Minimization and molecular dynamics simulations have been carried out on four complexes, HIV-1 Protease with Nelfinavir and subsequently with the new inhibitors, respectively, in order to analyze the behavior of the systems.

Additionally, we have calculated the binding free energy differences Protease:inhibitor, which gave us a quantitative idea of the new molecules inhibitory efficiency *in silico*.

Keywords: HIV-1 Protease; Nelfinavir; Binding free energy differences; Molecular dynamics; New inhibitors

1. Introduction

Since Acquired Immunodeficiency Syndrome (AIDS) was first described in the early 1980s, the worldwide epidemic has claimed the lives of 22 million people. Another 40 million live with HIV, the virus that causes AIDS.

HIV is a retrovirus that attacks the immune system with two primary types: HIV-1 and HIV-2. There are many strains of both types [1] and they all mutate rapidly, which has made it particularly difficult for researchers to find an effective vaccine [2] or treatment for the virus.

Although research is ongoing, no cure has yet been found for the disease. The most successful treatment currently known is a complex ''cocktail'' of drugs that attacks the virus at various stages of its lifecycle. These drugs include: Protease inhibitors, which slow down the virus maturation, reverse transcriptase inhibitors, which slow down the conversion of the viral RNA into double-stranded DNA, proper for integration in the cell DNA, and entry inhibitors, which inhibit viral entry to the cell.

HIV-1 Protease performs an essential step in the lifecycle of HIV. Like many viruses, HIV produces many of its proteins in one long piece, with several proteins strung together. HIV-1 Protease has the job of cutting this long 'polyprotein' into the proper protein-sized pieces. The timing of this step is critical. The intact polyprotein is necessary early in the life cycle, when it assembles the immature form of the virus. Then, the polyprotein must be cut into the proper pieces to form the mature virus, which can then infect a new cell. The cleavage reactions must be timed perfectly, allowing the immature virus to assemble properly before the polyprotein is divided. Because of its sensitive and essential function, HIV-1 Protease is an excellent target for drug therapy.

Even though there are many *in vitro* potent HIV-1 Protease inhibitors, only a few have advanced into clinical trials. Of these non-peptidic, relatively low molecular weight HIV-1 Protease inhibitors, Nelfinavir approved by FDA in 1997, has emerged as a combination of iterative structure-based drug design and an analysis of oral pharmacokinetics and antiviral activity [3].

Protease has been extensively studied and characterized through X-ray crystallography techniques. Protease is a homodimer (Chain A, Chain B), which is shown in Fig. 1 complexed with Nelfinavir. Nelfinavir itself is shown in Fig. 2.

* Corresponding author.
E-mail address: mjramos@fc.up.pt (M.J. Ramos).

1093-3263/$ – see front matter © 2007 Elsevier Inc. All rights reserved.
doi:10.1016/j.jmgm.2007.03.009

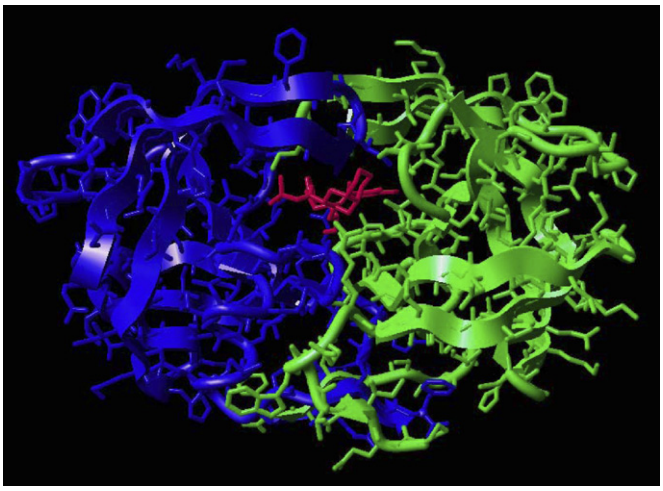

Fig. 1. Protease complexed with Nelfinavir.

Each monomer contains 99 amino acids and is identical in conformation. The folded subunits interact to form a hydrophobic core, a cylindrical cavity (24 Å long by 6–8 Å in diameter) and two flexible flaps (one per subunit) that can close around the substrate. Each flexible flap, 9 residues long (46–54), contains three characteristic regions: side chains that extend outward (Met46, Phe53), hydrophobic chains extending inward (Ile47, Ile54), and a glycine rich region (48, 49, 51, 52). Ile50 remains at the tip of the turn. A water molecule makes H bonds to the backbone of Ile50 of each monomer from the interior of the cleft when the protein is unliganded. This water molecule plays a role in the opening and closing of the flaps as well as increasing the affinity between enzyme and substrate. Centered in the hydrophobic active site are two symmetrically disposed catalytic aspartate residues (Asp25 and Asp25') that are involved in the hydrolysis of the peptide bond. Studies have shown that the hydrophobic cavern can hold eight amino acids of the substrate in an extended conformation for cleavage [4].

As mentioned beforehand, many crystal structures of HIV-1 Protease and its complexes with inhibitors have been solved, and extensive clinical resistance data have been accumulated in relation to the FDA and EMEA approved drugs throughout the years. Resistance mutations to the HIV-1 Protease drugs occur only at not well-conserved positions which interact more favorably with the drugs than with the substrate. More potent

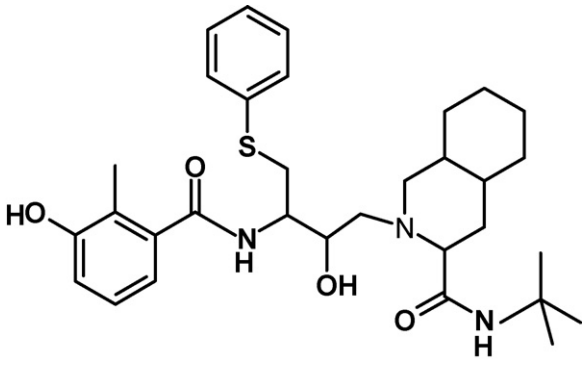

Fig. 2. Schematic representation of Nelfinavir.

Protease drugs should interact more favorably with well-conserved residues, which cannot undergo mutation at the cost of the enzyme to become catalytically inactive. From these, computational studies have identified the ones which have a more favourable profile for optimization [5]. Therefore, new inhibitors should become more efficient to combat HIV drug resistance if they interact more favorably with the well-conserved residues Leu23, Ala28, Gly49, Arg87, and more importantly, with Asp29.

In this work, we make a rational optimization of Nelfinavir, through chemical modifications that improve its performance, by increasing its affinity to well-conserved residues.

Molecular dynamics simulations in implicit solvent have been carried out on complexes of HIV-1 Protease with Nelfinavir and with the new inhibitors in order to study the behavior of the resulting systems.

Additionally, we have also calculated the binding free energies Protease:inhibitor, which provide a quantitative idea of the success of the complex association Protease:modified Nelfinavir.

2. Material and methods

2.1. The initial structure

Our starting structure of the complex Protease:Nelfinavir was obtained by fitting Nelfinavir into the Protease X-ray structure of the complex Protease:Amprenavir because the complex Protease:Nelfinavir X-ray structure presents 15 incomplete side chains.

The X-ray crystallographic structures of complexes Protease:Amprenavir and Protease:Nelfinavir were obtained in the database Protein Data Bank [6] with references 1HPV and 1OHR, respectively. In the choice of the structures, among others factors, their resolution was taken in account. The resolution of structures 1HPV and 1OHR is 1.90 and 2.10 Å, respectively.

One of the reasons why we have opted by fitting Nelfinavir into the Protease structure in the 1HPV file, instead of modelling the incomplete side chains in the 1OHR file, was because the root mean square deviation (rmsd) of the backbone of both Proteases was low, with a value of 0.73 Å. Additionally, both inhibitors are remarkably similar in shape and size with binding pockets that show the same conformation, with an all atom rmsd of 0.91 Å (all residues which have at least a heavy atom at less than 5 Å from the inhibitors were included in this calculation). Therefore, we have superimposed both crystallographic structures (Fig. 3), with the help of the software SwissPdbViewer [7], and replaced Amprenavir by Nelfinavir in the 1HPV structure.

Protons were added with the software GaussView [8], giving special attention to the hydrogen atoms added to the inhibitor.

It is known that only one of the two aspartate residues in Protease (residues 25, each one of chains A or B) is protonated. Even though it is not known which one of them is protonated, we assumed it was the one closer to the hydroxyl group of the non-scissile isostere, in agreement not only with the most

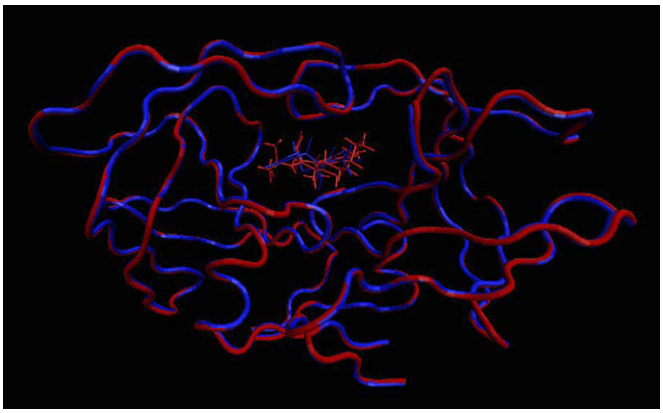

Fig. 3. Superposition of the 1OHR (red) and 1HPV (blue) structures, showing both active sites conformations and the binding mode of the Nelfinavir and Amprenavir inhibitors.

widely accepted catalytic scheme considered for the cleavage of the polyprotein by the Protease of HIV-1 [9], but also with our own findings which we shall specify at a later stage. Therefore, one hydrogen atom was added to aspartate 25 of chain B.

Even though the inhibitors are neutral we have calculated and used a charge of +5 for the Protease. It was verified that in the Protease the side chains of the His residues, frequently found in a non-standard protonation state ($pK_a = 6.1$), were exposed to the solvent, and therefore in a neutral state. Standard protonation states were assumed for all other residues.

2.2. New inhibitors

For the modifications introduced into Nelfinavir we used the GaussView [8] software.

Even though the shape complementarity between the Nelfinavir and the Protease is notorious, there is still room for further improvement, due to the existence of a set of small empty pockets between the inhibitors and the well-conserved amino acids. We performed chemical substitutions with appropriate size and polarity to establish interactions with the targeted amino acids.

To calculate the molecular electronic structures and properties for the new inhibitors we used Gaussian03 [10], performing restricted Hartree–Fock calculations (RHF), with the 6-31G(d) basis set, to be consistent with the parameterization adopted in Amber 8 [11], which was later used in the molecular dynamics calculations.

We used the Antechamber tools within Amber 8, in order to create an input file for modified Nelfinavir that could be read by Leap, another of Amber's modules. Antechamber is designed to be used with GAFF, the *general amber force field.* RESP [12] was the method used to calculate atomic charges.

2.3. Minimization and molecular dynamics

During the calculations, the solvent was modelled with a modified Generalized Born solvation model [13]. To release the bad contacts in the crystallographic structure the later was minimized in 3 stages: in the 1st stage only the hydrogen atoms added with xLeap were minimised, in the 2nd stage the backbone was also minimised, and in the 3rd and last stage, the entire system was minimized. About 1500 steps were used for each stage, with the first 500 steps performed using the steepest descent algorithm and the remaining steps carried out using conjugate gradient.

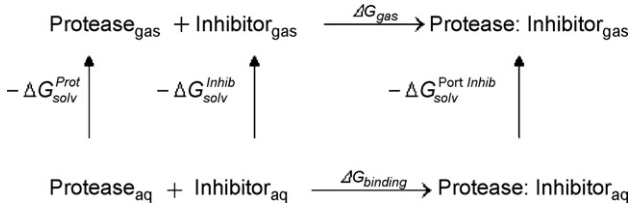

Fig. 4. Thermodynamic cycle used to calculate the binding free energy of all complexes Protease:inhibitor.

Subsequently, molecular dynamics (MD) simulations were performed starting from the minimized structures. All simulations presented in this work were carried out using the sander module, implemented in the Amber 8 [11] simulations package, with the *Cornell* force field [14]. Bond lengths involving hydrogens were constrained using the SHAKE algorithm [15], and the equations of motion were integrated with a 2 fs time-step using the Verlet leapfrog algorithm and the non-bonded interactions truncated with a 16 Å cutoff. The temperature of the system was regulated by the Langevin thermostat to maintain the temperature of our system at 310.15 K [16–18].

2.4. Calculation of binding free energies Protease:inhibitor

The MM_PBSA script implemented in Amber 8 [11] was used to calculate the binding free energies for all four complexes—Protease with Nelfinavir and Protease with the three new inhibitors. The MM_PBSA script [19] was used to perform a post processing treatment of the complex by using the structure of the complex, and calculating the respective energies for the complex and all interacting monomers. For the binding free energy calculations, 50 snapshots of the complexes were extracted every 50 steps for the last 2500 steps of the run.

The binding free energy can be calculated using the following thermodynamic cycle (Fig. 4):

The binding free energy difference between the Nelfinavir modified and Nelfinavir complexes is defined as:

$$\Delta\Delta G_{\text{binding}} = \Delta G_{\text{binding-modifing Nelfinavir}} - \Delta G_{\text{binding-Nelfinavir}}$$

The internal energy (bond, angle and dihedral), the electrostatic and the van der Walls interactions were calculated using the *Cornell* force field [14] with no cutoff. The electrostatic solvation free energy was calculated by solving the Poisson–Boltzmann equation with the software Delphi v.4 [20,21]. The accuracy of this method depends on the self-consistency of the model parameters used to solve the Finite Difference method implemented in DelPhi. The key parameters used were based in a detailed study of the effect of the variation of key parameters

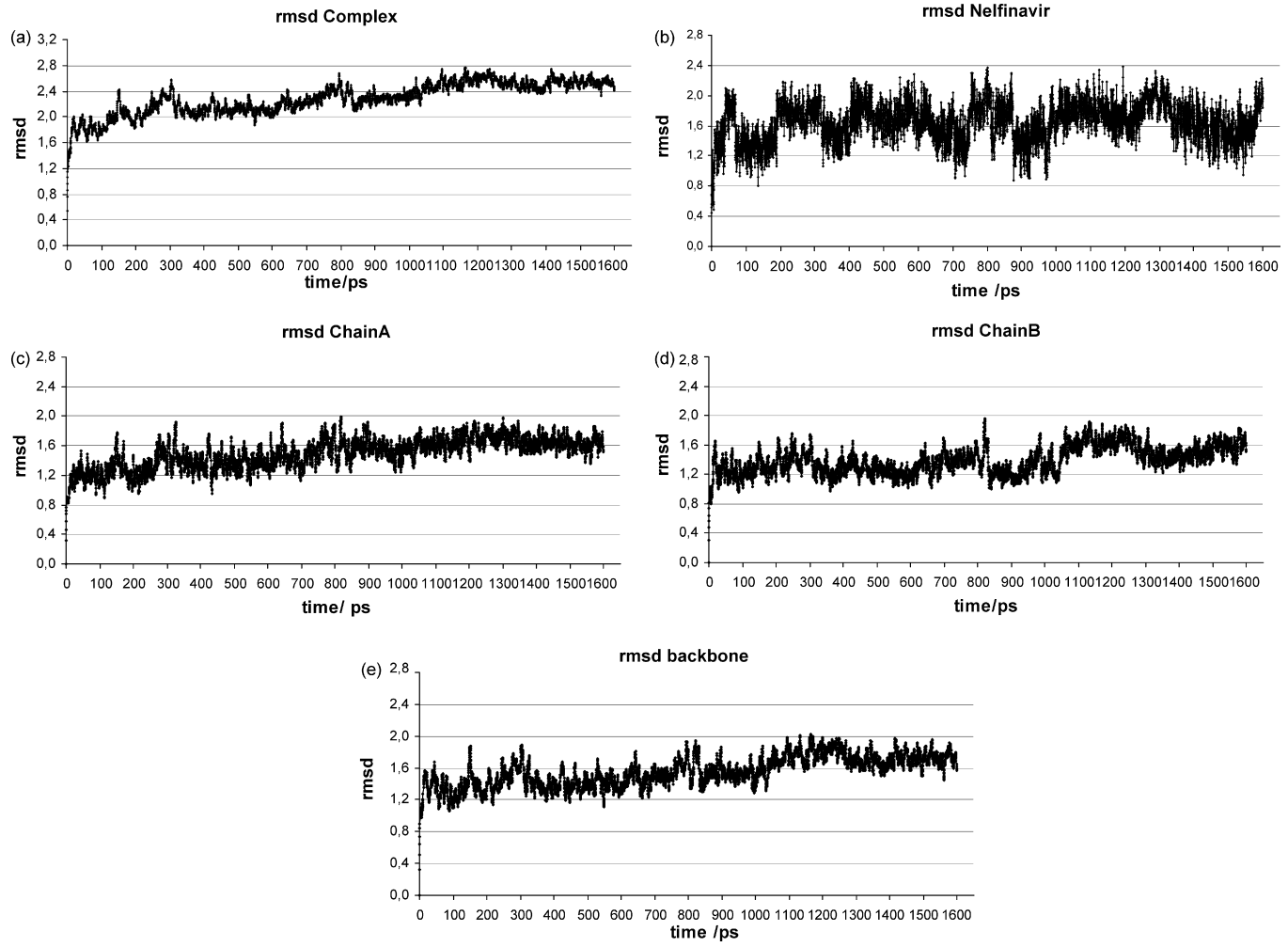

Fig. 5. rmsd of the trajectory structures as compared to the starting structures, for (a) complex Protease:Nelfinavir, (b) Nelfinavir, (c) Chain A of Protease, (d) Chain B of Protease and (e) backbone.

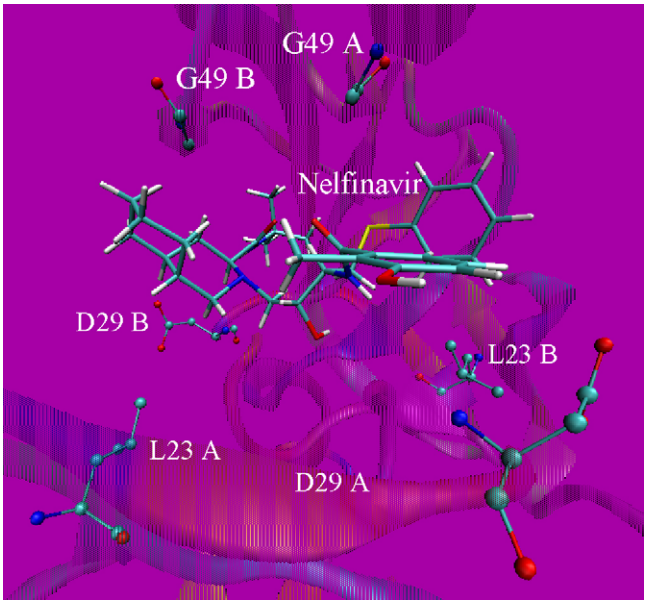

Fig. 6. Location of the well-conserved residues around Nelfinavir.

in several system as well as the correspondent computational time [22].

The non-polar contribution to solvation free energy due to van der Waals interactions between the solute and the solvent and cavity formation was modelled as a term that is dependent

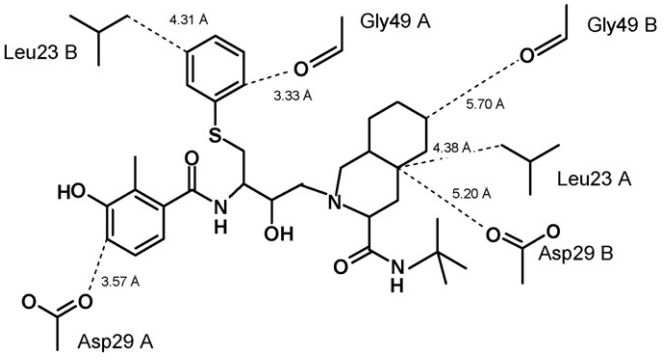

Fig. 7. Distances between well-conserved residues and the atoms in Nelfinavir where chemical substitutions are to be introduced. The distances have been measured in the structure resultant from the minimization of the complex Protease:Nelfinavir.

on the solvent accessible surface area of the molecule. It was estimated using an empirical relation:

$$\Delta G_{\text{nonpolar}} = o'A + \beta$$

where A is the solvent-accessible surface area that was estimated using the molsurf program, which is based on the idea primarily developed by Mike Connolly [23]. o' and β are empirical constants and the values used were 0.00542 kcal Å^{-2} mol^{-1} and 0.92 kcal mol^{-1} respectively. The entropy term was not calculated because it was assumed that its contribution to $\Delta\Delta G_{\text{binding}}$ is mainly cancelled and becomes negligible [19].

While the choice of the external dielectric constant depends on the solvent media, the choice of the internal dielectric constant has been the subject of discussion and controversy because the dielectric constant is not a universal constant but simply a parameter that depends on the model and the methodology used [19].

The value of the external dielectric constant used was 80.0. The value of the interior dielectric constant was set to 1.25. It was a cautious and rational choice, because with this value and the present protocol we can reproduce computationally the binding free energy of Nelfinavir obtained from experimental procedures, (−13 kcal/mol) [5]. This value takes advantage of error cancellation and gives a more accurate picture of the values from the substitutions.

3. Results and discussion

3.1. Protease:Nelfinavir complex

Nelfinavir presents a potent antiviral activity and an extraordinary complementarity towards the binding pocket of HIV-1 Protease. It has a molecular mass of 567.8 amu, has four hydrogen bonds donors and four hydrogen bonds acceptors, has very favourable ADMET profile and is orally bioavailable [24].

However, the long-term efficiency of Nelfinavir is limited by the capacity of the virus to develop mutations which decrease binding to Protease, becoming imperative the development of more efficient inhibitors. Studies about resistance mutations show that new inhibitors should interact more favourably with well-conserved residues Leu23, Ala28, Gly49, Arg87, and Asp29 [5].

To study the behaviour of the system Protease:Nelfinavir, after minimizing the 3D-structure in three stages, we performed a 1600 ps molecular dynamics simulation of the system in implicit solvent.

To assess the quality of the simulations, we monitored the root mean square deviations of the trajectory structures as compared to the starting structure for the complex Protease:-Nelfinavir, for Nelfinavir itself, for each monomer of Protease (chains A and B), and for the backbone. The rmsds are shown in Fig. 5.

Inspection of the rmsd and the potential energy profiles allowed us to verify that equilibration was achieved.

It is important to highlight that the rmsd value for Nelfinavir, that subsequentely was the target of chemical modifications did not exceed 2.4 Å. Such value, as well as the small oscillations in the rmsd value verified throughout the trajectory are mainly related to the fact that the aromatic ring, linked to the sulphur atom, is very flexible and can occupy several different rotamers.

Although Nelfinavir shows an extraordinary specificity to the binding pocket of HIV-1 Protease, the shape and size complementarity are not perfect, and by analysing the crystallographic structure one can see that there is still room for further improvement. A small set of empty pockets between Nelfinavir and the most conserved residues allows the introduction of small chemical groups that increase the binding without decreasing the oral efficiency.

Even though five residues were identified as a possible target for improving the affinity to Protease we have excluded two of them, Ala28 and Arg87.

Ala28 was excluded due to its hydrophobic nature and the fact that it is close to two other hydrophobic residues with high variability, Val32 and Ileu84, known to mutate upon drug administration, and therefore substitutions tend to interact unspecifically with the three side chains, making the substitutions more prone to induce the development of resistance.

Arg87 was excluded because it is located at a distance of 8 Å from the inhibitor in a position which can be perceived as a ''second shell'' of residues around the inhibitors—all the other well-conserved residues are located in a first shell of residues. Moreover, Asp29 is located between Arg87 and Nelfinavir. Due to the large Arg87-inhibitors distance, only long-range electrostatic interactions could be invoked to improve affinity. However, such substitutions (groups of negative polarity/charge in the inhibitors) will interact unfavourably with Asp29, which is between them and much closer to the inhibitor, generating a much stronger repulsion than the attraction due to Arg87.

Fig. 6 shows the 3D location of the well-conserved residues around Nelfinavir. Fig. 7 shows a schematic representation of the binding region for Nelfinavir with which the substitutions introduced in the inhibitors are meant to interact. The dashed lines give an idea of the location of the empty pockets between the well-conserved amino acids and the inhibitors.

Between Nelfinavir and these residues there are no other atoms. Therefore, the small empty cavities can be filled with appropriate substitutions without generating steric collisions with other parts of the enzyme.

To evaluate the binding affinity of the inhibitors we have used MM_PBSA [19]. This method explores the type of established interactions, calculating separately the components of the internal energy, the interaction energy and the free energy of Gibbs of solvation.

The values for the binding free energy presented in Table 1 are validated by the correct reproduction of the experimental values. From experimental procedures, the value obtained for the Protease:Nelfinavir complex, (pH 6.5), is −13 kcal/mol. We have calibrated the internal dielectric constant for the active site against the experimental $\Delta G_{\text{binding}}$ having obtained −12.6 kcal/mol for the latter with a dielectric constant of $\varepsilon = 1.25$. This value accounts for the lack of polarizability of the force field,

Table 1
Values of the free energy of Gibbs for Nelfinavir and new inhibitors, all values in kcal/mol

	ΔE_{int}^{ele}	ΔE_{int}^{vdw}	ΔG^{nonpol}	ΔG_{sol}^{ele}	$\Delta G_{int+sol}^{ele}$	ΔG_{bind}	$\delta\Delta G_{bind}$	$\Delta\Delta G_{bind}$
Nelfinavir	−13.6	−58.8	−7.63	67.4	53.8	−12.6	0.8	0.0
Inhibitor 1	−12.3	−54.6	−7.74	55.2	42.9	−19.5	0.8	−6.9
Inhibitor 2	−10.8	−61.7	−8.05	55.9	45.2	−24.6	0.8	−12.0
Inhibitor 3	−11.3	−58.5	−7.71	60.3	48.9	−17.2	1.0	−4.6

ΔE_{int}^{ele}, internal interaction free energy electrostatic; ΔE_{int}^{vdw}, internal interaction free energy of van der Walls; ΔG^{nonpol}, free energy non-polar, ΔG_{sol}^{ele}, solvation free energy electrostatic; $\Delta G_{int+sol}^{ele}$, the internal interaction and solvation free energy electrostatic; ΔG_{bind}, binding free energy; $\delta\Delta G_{bind}$, rms deviation in binding free energy; $\Delta\Delta G_{bind}$, binding free energy difference.

systematic inaccuracies inherent to the force field parameters and energy equation, and incomplete sampling of the configurational space, and gives a more accurate picture of the $\Delta\Delta G_{binding}$ values for the substitutions. Additionally, the system resulting from Protease when bound is asymmetric, giving different ΔG values when chains A or B are protonated. With the chain B protonated we have obtained a ΔG value very close to the experimental one and certainly in within the experimental error. Therefore, one hydrogen atom was added to aspartate 25 of chain B.

Inhibitors 1, 2 and 3 which will be described in the next sections are the result of successful substitutions introduced onto Nelfinavir.

To study the behaviour of each system Protease:inhibitor, after minimizing the 3D-structures in three stages, we performed molecular dynamics simulations in implicit solvent.

To assess the quality of the simulations, we monitored the root mean square deviations of the trajectories comparing structures to the starting structures for the complex, the inhibitors, each monomer of the Protease (chains A and B), and the backbone.

To evaluate the inhibitory efficiency, the values of the free energy of Gibbs are calculated and compared with the ones obtained for Nelfinavir (Table 1).

3.2. Inhibitor 1

The complementarity of Nelfinavir to the oxygen atom of the Asp29 B is extremely poor. The oxygen, polar and charged, interacts with the hydrophobic ring at a distance of 5.20 Å. That ring establishes hydrophobic interactions with the side chain of Leu23 A. However, it is still possible increase the vdW interactions with this group.

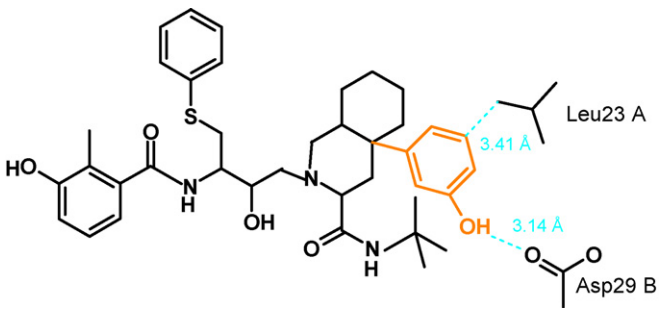

Fig. 8. Schematic representation of inhibitor 1. In orange, the group added onto Nelfinavir.

A phenyl group introduction in the axial position with a *meta*-hydroxyl group has an appropriate size for the cavity, possesses groups with adequate polarity to establish hydrogen bonds with the carboxylate group and vdW interactions with Leu23.

Fig. 8 features the modelling of an aromatic ring, to interact with both amino-acids, which confers conformational rigidity, specificity and low binding entropic cost for the inhibitor.

Inspection of the rmsd and the potential energy profiles allowed us to verify that equilibration was achieved (see supporting information for the rmsd graphics of the corresponding trajectory structures).

The calculated difference in the binding free energy, $\Delta\Delta G_{bind} = -6.9 \pm 1.1$ kcal/mol (Table 1, column9), indicates that inhibitor 1 has a higher affinity to Protease than Nelfinavir. However, only the electrostatic part is favoured. Nelfinavir establishes a vdW short-range interaction with Leu23, and the addition of a volumous group brings together excessively two hydrophobic groups. On the other hand, the establishment of a hydrogen bridge with Asp29 B contributes favourably to the increase of the inhibitory efficiency.

Fig. 9 shows details of the interaction between the Protease conserved residues, Leu23 A and Gly49 B, and inhibitor 1. The presented structure is one of the equilibrated structures of the simulation.

The conformational similarity of the Proteases in the two systems was also verified and confirmed. We superimposed the

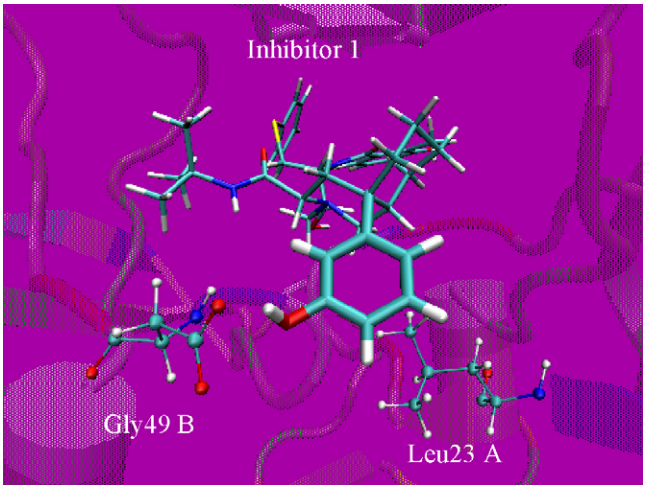

Fig. 9. Interaction between inhibitor 1 and the conserved residues, Leu23 A and Gly49 B of Protease. The group added to Nelfinavir is shown in bold.

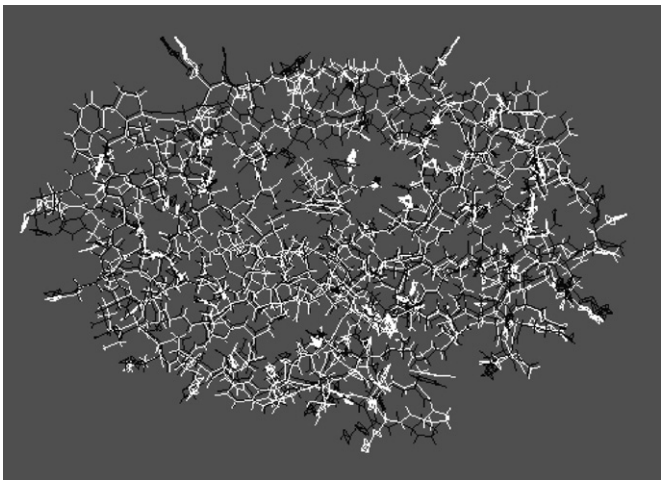

Fig. 10. The overlapping of the two Proteases in the complexes Protease:Nelfinavir (black) and Protease:inhibitor 1 (white).

average structure of complex Protease:Nelfinavir with the average structure of complex Protease:inhibitor 1 and the rmsd of the backbone of both Proteases was 1.03 Å. Therefore, the enzyme did not suffer significant conformational changes. The Figure 10 illustrates the overlapping of the Proteases in both complexes Protease:Nelfinavir and Protease:inhibitor 1.

The introduction of one more hydrogen donor group in the molecule increases to 5 the total number of hydrogen donors, a number still within the Lipinski rules, which points to a maximum number of five hydrogen bond donors as a requisite for good absorption and permeation properties [24]. The increase in the molecular mass of the inhibitor is 98.1 amu. It is well known that permeation decreases steadily with the molecular mass, and poor permeation is the usual scenario for drugs above 500 amu Nelfinavir, as well as all the other bioavailable Protease inhibitors, are exceptions to this picture as all of them possess oral activity with molecular masses well above 500 amu Nelfinavir is one of the Protease antiretrovirals with lower molecular mass, 567.8 amu, and therefore the increase in the molecular mass due to the substitutions should not compromise its oral availability.

In conclusion, inhibitor 1 presents greater inhibitory efficiency than Nelfinavir.

3.3. Inhibitor 2

The phenyl ring (that is bound to the Nelfinavir scaffold by the sulphur atom) establishes favourable hydrophobic interactions with the conserved residue Leu23 B. The closest distance between a phenyl carbon and the side chain of Leu23 B corresponds to 4.31 Å. Therefore, it is still possible to increase the vdW interactions between these two groups. Due to the close proximity we considered the introduction of an ethyl group in the ring (Fig. 11).

The closest distance between the ring carbon and the backbone carbonyl oxygen of Gly49 A corresponds to 3.33 Å. The introduction of appropriate small-size hydrogen bond donors, which would establish an hydrogen bond with this

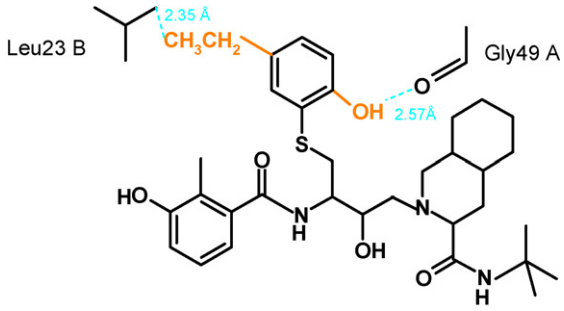

Fig. 11. Schematic representation of inhibitor 2. In orange, the groups added onto Nelfinavir.

extremely conserved residue, (Gly49), should lead to an increase in affinity (Fig. 11).

The $\Delta\Delta G_{bind}$ value, -12.0 ± 1.1 kcal/mol, indicates that inhibitor 2 has a higger affinity for Protease than Nelfinavir. As we can observe in Table 1, this inhibitor presents an increase in the electrostatic and the vdW interactions.

Inspection of the rmsd and the potential energy profiles allowed us to verify that equilibration was achieved (see supporting information for the rmsds of the corresponding trajectory structures).

The formation of a hydrogen bridge with Gly49 A contributes favourably for affinity. Throughout the molecular dynamic simulation, the oxygen of the hydroxyl group added is obviously in the plane of the ring even though the hydrogen rotates almost freely along the H–O–C–C dihedral.

It was verified that no significant interactions are established with Gly48, an extremely changeable residue, whose substitutions for it directed will be able to induce resistance.

Throughout the dynamics the very flexible ethyl group added, sometimes interacts with Leu23 A sometimes is next Leu23 B.

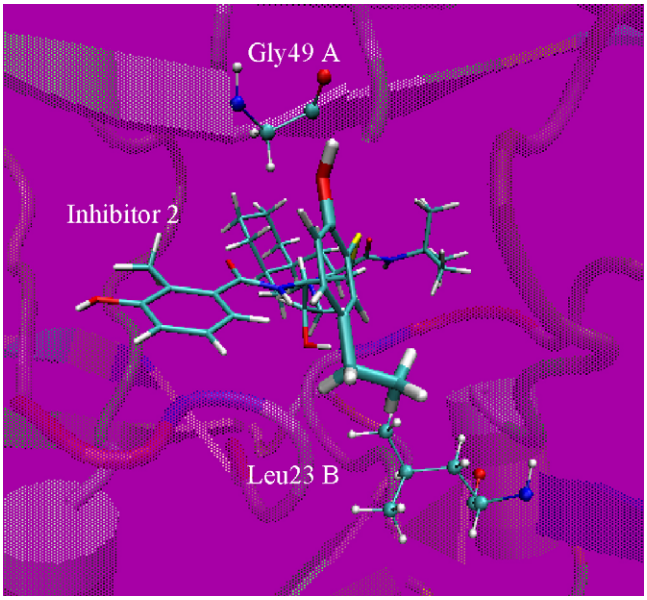

Fig. 12. Interaction between inhibitor 2 and the conserved residues, Leu23 B and Gly49 A, of Protease. Groups added onto Nelfinavir are shown in bold.

Fig. 12 shows details of the interaction between the Protease conserved residues, Leu23 B and Gly49 A, and inhibitor 2. The structure presented is one of the equilibrated structures of the simulation.

The conformational similarity of the Proteases was confirmed. We have superimposed the average structure of the complex Protease:Nelfinavir and the average structure of the complex Protease:inhibitor 2 and the rmsd of the backbone was 0.91 Å. The enzyme did not suffer significant changes (the overlapping of the Proteases in both complexes Protease:Nelfinavir and Protease:inhibitor 2 can be seen in supporting information).

The increase in molecular mass is small, the inclusion of one more hydrogen bond donor does not overcome the Lipinsky rules [24], and therefore the pharmacologic properties are not expected to be affected. Inhibitor 2 should really be more efficient.

3.4. Inhibitor 3

The polar complementarity between the phenyl carbon and the carboxylate oxygen of Asp29 A is extremely poor. The ionic carboxylate interacts with the hydrophobic ring to a distance of 3.57 Å. Such interaction is not competitive with the solvation of the charged residue and contributes unfavourably to affinity. The introduction of an hydroxyl group, a small-size hydrogen bond-donor, will result in a establishment of a charged hydrogen bond with the carboxylate of Asp29 A leading to an increase in affinity.

The closest distance between a phenyl carbon and a methyl group of the side chain of Leu23 B is 4.01 Å. It is still possible to increase the vdW interactions between these two hydrophobic groups. Due to the close proximity, only a methyl group was considered possible introduce.

Fig. 13 features the groups added onto Nelfinavir.

The $\Delta\Delta G_{bind}$ value, -4.6 ± 1.3 kcal/mol, indicates that inhibitor 3 has a higher affinity for the Protease than Nelfinavir. As we can observe in Table 1, this inhibitor presents an increase in the electrostatic interactions and is similar to the Nelfinavir as far as the vdW interactions are concerned.

The increase verified in the electrostatic interactions is smaller than expected. This is because the hydroxyl group

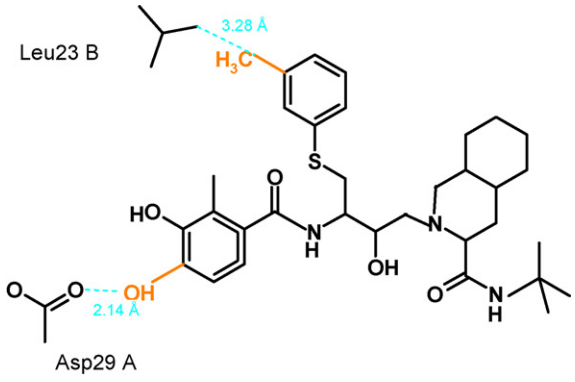

Fig. 13. Schematic representation of inhibitor 3. In orange, the groups added onto Nelfinavir.

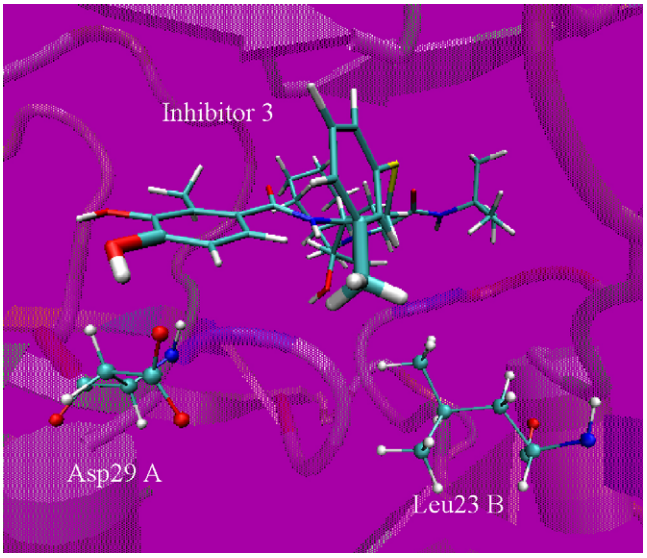

Fig. 14. Interaction between inhibitor 3 and the conserved residues, Leu23 B and Asp29 A, of Protease. Groups added onto Nelfinavir are shown in bold.

added establishes intramolecular interactions with the neighbouring hydroxyl group. The visualization of the some structures of the complex throughout the simulation and the analyses of the rmsd charts allowed us to verify that equilibration was achieved and the rmsd value for inhibitor 3 did not exceed 2.6 Å.

Fig. 14 shows the details of the interaction between the enzyme and inhibitor 3. The structure presented is one of the equilibrated structures of the simulation.

The conformational similarity of the Proteases was confirmed. We overlapped the average structure of the complex Protease:Nelfinavir with the average structure of complex Protease:inhibitor 3 and the rmsd of the backbone of both Proteases was 0.76 Å. Therefore, the enzyme did not suffer significant conformational changes. The overlapping of the Proteases in both complexes Protease:Nelfinavir and Protease:inhibitor 3 can be seen in supporting information.

The increase in the molecular mass is small, and the substitutions should preserve good ADME properties. In conclusion, inhibitor 3 presents greater inhibitory efficiency to Protease than Nelfinavir.

4. Conclusion

Three newly designed inhibitors have been presented here which have *in silico* a higher affinity for Protease than Nelfinavir. This was justified quantitatively with calculated values of the binding free energy differences and qualitatively through the new interactions that were observed between the new inhibitors and Protease. It would be interesting to find out a relationship between these new inhibitors and SAR/QSAR analysis of Nelfinavir. However, we could not find in the literature maybe because drug companies cannot afford to publish their most interesting results [25]. The inhibitors do not include an excessive number of hydrogen bridges donors and acceptors, nor a significant increase in the molecular mass in

relation to Nelfinavir. It is expected that inhibitors 1, 2 and 3 will combine its same ADME properties with an increase in affinity and specificity and a higher resistance to mutations.

Appendix A. Supplementary data

Supplementary data associated with this article can be found, in the online version, at doi:10.1016/j.jmgm.2007.03.009.

References

[1] A. Rambaut, D. Posada, K.A. Crandall, E.C. Holmes, Nat. Rev. Gen. 5 (2004) 52–61.
[2] C. Dennis, Nature 421 (2003) 877–878.
[3] S.W. Kaldor, V.J. Kalish, J.F. Davies II, B.V. Shetty, J.E. Fritz, K. Appelt, J.A. Burgess, K.M. Campanale, N.Y. Chirgadze, D.K. Clawson, B.A. Dressman, S.D. Hatch, D.A. Khalil, M.B. Kosa, P.P. Lubbehusen, M.A. Muesing, A.K. Patick, S.H. Reich, K.S. Su, J.H. Tatlock, J. Med. Chem. 40 (1997) 3979–3985.
[4] M. Prabu-Jeyabalan, E. Nalivaika, C.A. Schiffer, J. Mol. Biol. 301 (2000) 1207–1220.
[5] W. Wang, P.A. Kollman, PNAS 98 (2001) 14937–14942.
[6] http://www.rcsb.org/pdb.
[7] N. Guex, M.C. Peitsch, Electrophoresis 18 (1997) 2714–2723. http://www. expasy. org/spdbv/.
[8] Gaussian Inc., Carnegie Office Park, Bldg. 6, Pittsburgh, PA 15106, USA.
[9] S. Piana, D. Bucher, P. Carloni, U. Rothlisberger, J. Phys. Chem. B 108 (2004) 11139–11149.
[10] M.J. Frisch, G.W. Trucks, H.B. Schlegel, G.E. Scuseria, M.A. Robb, J.R. Cheeseman, J.A. Montgomery Jr., T. Vreven, K.N. Kudin, J.C. Burant, J.M. Millam, S.S. Iyengar, J. Tomasi, V. Barone, B. Mennucci, M. Cossi, G. Scalmani, N. Rega, G.A. Petersson, H. Nakatsuji, M. Hada, M. Ehara, K. Toyota, R. Fukuda, J. Hasegawa, M. Ishida, T. Nakajima, Y. Honda, O. Kitao, H. Nakai, M. Klene, X. Li, J.E. Knox, H.P. Hratchian, J.B. Cross, V. Bakken, C. Adamo, J. Jaramillo, R. Gomperts, R.E. Stratmann, O. Yazyev, A.J. Austin, R. Cammi, C. Pomelli, J.W. Ochterski, P.Y. Ayala, K. Morokuma, G.A. Voth, P. Salvador, J.J. Dannenberg, V.G. Zakrzewski, S. Dapprich, A.D. Daniels, M.C. Strain, O. Farkas, D.K. Malick, A.D. Rabuck, K. Raghavachari, J.B. Foresman, J.V. Ortiz, Q. Cui, A.G. Baboul, S. Clifford, J. Cioslowski, B.B. Stefanov, G. Liu, A. Liashenko, P. Piskorz, I. Komaromi, R.L. Martin, D.J. Fox, T. Keith, M.A. Al-Laham, C.Y. Peng, A. Nanayakkara, M. Challacombe, P.M.W. Gill, B. Johnson, W. Chen, M.W. Wong, C. Gonzalez, J.A. Pople, Gaussian 03 Inc., Revision B.04 ed., Pittsburgh, PA, 2003.
[11] D.A. Case, T.A. Darden, T.E. Cheatham III, C.L. Simmerling, J. Wang, R.E. Duke, R. Luo, H.M. Merz, B. Wang, D.A. Pearlman, M. Crowley, S. Brozell, V. Tsui, H. Gohlke, J. Mongan, V. Hornak, G. Cui, P. Beroza, C. Schafmeister, J.W. Caldwell, W.S. Ross, P.A. Kollman, AMBER 8, University of California, San Francisco, 2004.
[12] C.I. Bayly, P. Cieplak, W. Cornell, P.A. Kollman, J. Phys. Chem. 97 (40) (1993) 10269–10280.
[13] V. Tsui, D.A. Case, Biopolymers (Nucleic Acid Sci.) 56 (2001) 275.
[14] W.D. Cornell, P. Cieplak, C.I. Bayly, I.R. Gould, K.M. Merz, D.M. Ferguson, D.C. Spellmeyer, T. Fox, J.W. Caldwell, P.A. Kollman, J. Am. Chem. Soc. 117 (1995) 5179.
[15] J.P. Ryckaert, G. Ciccotti, H.J. Berendsen, J. Comput. Phys. 23 (1997) 327.
[16] I.W.R. Pastor, B.R. Brooks, A. Szabo, J. Mol. Phys. 65 (1998) 1409.
[17] R.J. Loncharich, B.R. Brooks, R.W. Pastor, Biopolymers 32 (1992) 523.
[18] J.A. Izaguirre, D.P. Catarello, J.M. Wozniak, R.D. Skeel, J. Chem. Phys. 114 (2001) 2090.
[19] S. Huo, I. Massova, P.A. Kollman, J. Comput. Chem. 23 (2002) 15.
[20] W. Rocchia, S. Sridharan, A. Nicholls, E. Alexov, A. Chiabrera, B. Honig, J. Comput. Chem. 23 (2002) 128.
[21] W. Rocchia, E. Alexov, B. Honig, J. Phys. Chem. B 105 (2001) 6507.
[22] I.S. Moreira, P.A. Fernandes, M.J. Ramos, J. Mol. Struct. (Theochem.) 729 (2005) 11.
[23] M.L. Connolly, J. Appl. Cryst. 16 (1983) 548.
[24] C.A. Lipinski, F. Lombardo, B.W. Dominy, P.J. Feeney, Adv. Drug Deliv. Rev. 46 (2001) 3–26.
[25] R. Garg, P.S. Gupta, H. Gao, M.S. Babu, A.K. Debnath, C. Hansch, Am. Chem. Soc. 99 (1999) 3525–3601.